Quasi-Luenberger Observer-Based Robust DC Link Control of UIPC for Flexible Power Exchange Control in Hybrid Microgrids

Zolfaghari, Mahdi ; Gharehpetian, Gevork B. ; Anvari-Moghaddam, Amjad

Published in:
I E E E Systems Journal

DOI (link to publication from Publisher):
10.1109/JSYST.2020.2991653

Publication date:
2021

Document Version
Accepted author manuscript, peer reviewed version

Quasi-Luenberger Observer-Based Robust DC Link Control of UIPC for Flexible Power Exchange Control in Hybrid Microgrids

Mahdi Zolfaghari, *Member, IEEE*, Gevork B. Gharehpetian, *Senior Member, IEEE*, and Amjad Anvari-Moghaddam, *Senior Member, IEEE*

***Abstract*—This work illustrates the application of an observer-based robust control of unified interphase power controller (UIPC) for power flow control between interconnected microgrids in hybrid microgrids. Here, the challenges of UIPC control in heterogeneous structure of hybrid microgrid are addressed, and a new control scheme for UIPC is proposed. In the proposed control scheme, the states of the UIPC dc link nonlinear dynamics are estimated using a Quasi-Luenberger observer. Then, the estimated states are implemented in a robust sliding mode controller that alleviates the effect of disturbances on the dc link dynamics and effectively controls the dc side power converter of the UIPC. The simulation results and comparison studies are provided to validate the efficacy of the proposed control scheme for hybrid microgrid.**

***Index Terms*—Hybrid microgrid, Quasi-Luenberger observer, sliding mode control, unified interphase power controller (UIPC).**

I. Introduction

FOR the future power systems, microgrid will be a key element to smoothly control and manage renewable energy sources (RESs) and loads [1]. A microgrid is characterized as a small-scaled low voltage system, which can operate in islanding mode or is embedded in electric distribution system, and contains different energy resources and loads with a control strategy [2], [3]. There are three types of microgrids: ac microgrids, dc microgrids, and hybrid ac–dc microgrids. Both ac and dc microgrids have been well studied in literature and the research continues in this type of microgrids and different control strategies with various control objectives have been presented by the researchers. For example, recently in [4], a semiconsensus control algorithm has been proposed to multifunctionally control the hybrid energy resources in dc microgrids. Also, a distributed control strategy has been described in [5] to control thermostatically-controlled loads in microgrids. Considering an islanded microgrid, Wang *et al.* [6] have developed an event-triggered secondary control algorithm for microgrids. As reported, the hybrid microgrids, which are a combination of ac and dc microgrids, are the most dominant type structures that will be used in future smart grids [7]. A hybrid microgrid includes at least two microgrids that conventionally have been connected together using parallel-connected interlink power converters (ILCs) to exchange power. Each microgrid contains energy resources and related loads. The RESs in microgrid may include wind turbines and photovoltaic (PV) systems, and the loads would be ac, dc, or of both types. The ILCs have commonly been used to interconnect microgrids; however, there are some technical issues in paralleling the power converters in hybrid microgrids. First, the dc link of all of the power converters is common. This makes the decoupled active and reactive power control more challenging [8]. Second, the dc link voltage oscillations affect the active power exchange between the dc and ac sides. This may cause instability and abrupt loss of the power exchange performance [9]. Third, if a short-circuit fault occurs at the dc or ac side, the current passing through an ILC may exceeds its rating, causing the outage of the ILC and loss of exchanged power [8], [9].

To resolve these issues, different approaches have been described in literature. A hierarchical control scheme for parallel-connected bidirectional ILCs has been described in [10]. In [11], a fault-protected active power control scheme has been proposed for grid-connected hybrid microgrids. The method uses a tunable scalar to vary the magnitude of active and reactive power oscillations. The framework of the control scheme, neglecting coupled components, has been implemented in stationary reference frame. A droop control-based hierarchical control scheme has been introduced in [12]. In the dc side, the proportional-integral (PI) controllers have been implemented whereas the proportional-resonant controller have been used at the ac side. Wang *et al.* [13] have indicated that the voltage unbalance results in power fluctuations. A control strategy for parallel-connected ILCs has been proposed, which controlled the current of each power converter so that the summation of the currents of all ILCs was balanced. To this end, one of the ILCs is considered as "redundant" with higher ratings. This makes the control scheme costly. Also, the proposed method is weak against harmonic distortion and moreover, the scheme is unable to reduce the reactive power oscillations. The observer-based control strategies have also been proposed in many applications.

Manuscript received January 23, 2020; revised March 31, 2020; accepted April 28, 2020. The work of M. Zolfaghari and G. B. Gharehpetian has been supported by the Elite National Foundation of Iran. *(Corresponding author: Amjad Anvari-Moghaddam.)*

Mahdi Zolfaghari and Gevork B. Gharehpetian are with the Electrical Engineering Department, Amirkabir University of Technology, Tehran 1591634311, Iran (e-mail: mahdizolfaghari@aut.ac.ir; grptian@aut.ac.ir).

Amjad Anvari-Moghaddam is with the Department of Energy Technology, Aalborg University 9220, Aalborg, Denmark (e-mail: aam@et.aau.dk).

Digital Object Identifier 10.1109/JSYST.2020.2991653

In [14], a distributed observer and controller have been designed for spatially interconnected systems. An observer-based nonlinear control scheme for transient stabilization of power system using sliding mode control strategy has been presented in [15]. Tummala *et al.* [16] have presented an observer based sliding mode frequency control for multimachine power systems with high penetration level of renewable energy resources. In [17], a perturbation observer based multiloop control scheme has been presented for the doubly-fed induction generator-wind turbine (DFIG-WT) in multimachine power systems. More recently, a new observer-based control scheme for dc link control of power converters has been proposed in [7], [18], and [19].

The unified interphase power controller (UIPC) has been proposed in [20] to control active and reactive power in power systems. As described in [20], the UIPC has the merits of interphase power controller and the unified power flow controller simultaneously. The UIPC can provide flexible power flow control, inherent fault current limiting capability, voltage isolation, and ac voltage regulation. The UIPC has previously been used in some power system applications. In [21] the transient stability of a grid-connected wind farm has been enhanced using the UIPC. Firouzi *et al.* [22] have used the UIPC to limit the sort-circuit current and power flow control of wind units.

More recently, in [18], a modified model of UIPC has been proposed, which in comparison to the model described in [20], implements a smaller number of power converters in its structure. This new model then has been used for interconnection of ac and dc microgrids in a grid-connected hybrid microgrid [18]. This is an effective alternative for parallel-connected power converters (ILCs) that have been used conventionally to interconnect dc and ac microgrids. It has been indicated in [18] that this topology has been able to provide a smooth power exchange control between ac and dc microgrids. Besides that, the problems raised by the conventional ILCs have been avoided. The dc link of the UIPC is connected to the common dc bus of the dc microgrid. However, because there are intermittent renewable sources, such as PV systems, the dc link voltage is fluctuating. This causes power flow oscillations and partially has been alleviated using a control technique described in [18]. Therefore, the dc link voltage can fluctuate and as a result, damping these fluctuations is mandatory for the UIPC to have a stable operation.

Aiming on removing aforementioned problems, this article presents a comprehensive nonlinear dynamic modelling of the dc link of the modified model of UIPC with an observer-based dc link control scheme. A Quasi-Luenberger observer is implemented to estimate the dc link dynamics. This observer removes the extra measurement links that are mandatory in traditional dc link control schemes and furthermore, it facilitates realization of the plug-and-play feature for the microgrids. Then, a robust sliding mode controller (SMC) is designed to counteract with these disturbances. For an uncertain and perturbed system, such as the dc link dynamics considered here, the conventional controllers, for example, the PI controllers, could not provide stable operation. The advantages of SMC can be numerated as follows.

1) *Speed:* Sliding mode (SM) control can be designed to be much faster than other conventional methods in case of many systems.

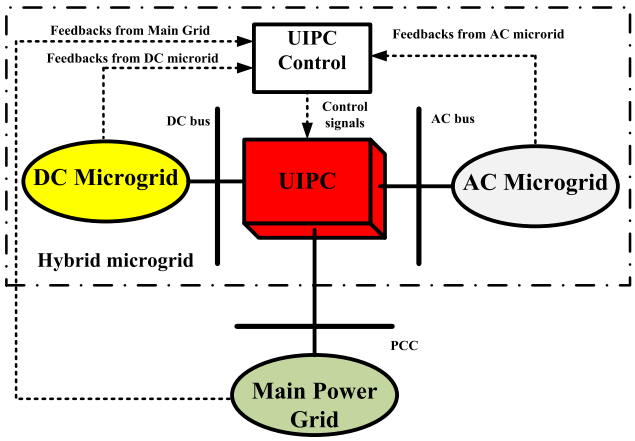

Fig. 1. Hybrid microgrid interconnected using UIPC.

2) *Nonlinearity:* By its nature, SM control can be appropriate for many severely nonlinear systems that may not be open to linearization in the first place, such as by using exact feedback linearization.
3) *Switching nature:* Certain technologies, by their nature, are well suited to control that employ *switching*. A good bunch of examples can be found in power electronic circuits, which are by their nature, *switching circuits*, as it is in this article.

Therefore, the main contributions of this article are as follows.

1) Addressing the challenges of UIPC dc link control in heterogeneous structure of hybrid microgrid.
2) Presenting the nonlinear dynamic model of dc link of UIPC.
3) Proposing a new robust dc link control scheme for UIPC based on a new Quasi-Luenberger observer.

The remainder of this article is organized as follows. Section II describes the hybrid microgrid structure and the modified UIPC model together with the nonlinear dynamics of the UIPC dc link. The application of Quasi-Luenberger state observer to the nonlinear dynamic model of the dc link and designing the robust SMC are detailed in Section III. The simulation results are given in Section IV and finally, Section V concludes this article.

II. Hybrid Microgrid Topology and Dynamic Model

Fig. 1 shows the overall diagram of the hybrid microgrid structure which uses the UIPC to connect the microgrids. As shown, the common ac bus and point of common coupling (PCC), are interconnected through the UIPC. The dc link of the UIPC is supplied through the dc microgrid. In this topology, two microgrids are able to exchange power with each other and also with the main power grid. Since the hybrid microgrid is connected to the main grid, the voltage and frequency are controlled by the utility [18]. Therefore, the UIPC is responsible for controlling the exchanged power among the microgrids and main grid.

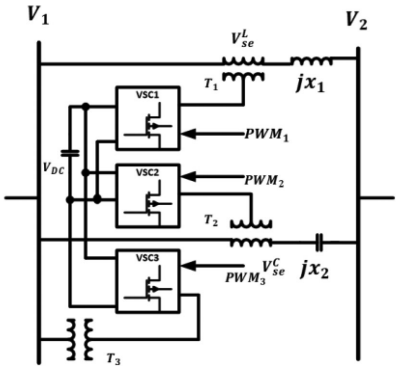

Fig. 2. Conventional topology of UIPC [20].

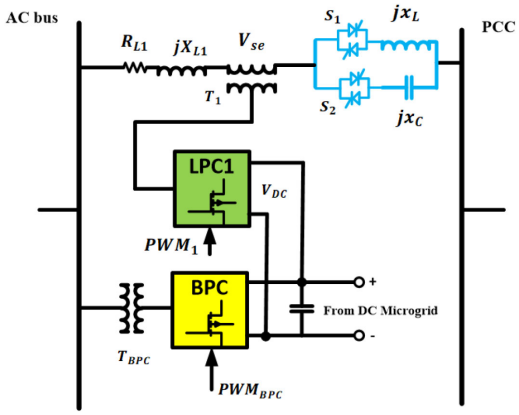

Fig. 3. Modified UIPC topology.

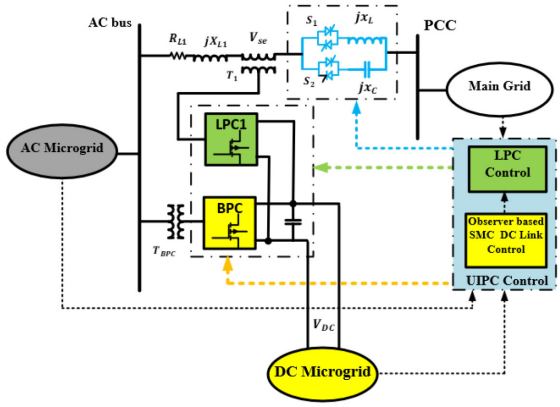

Fig. 4. Overall diagram of proposed control strategy.

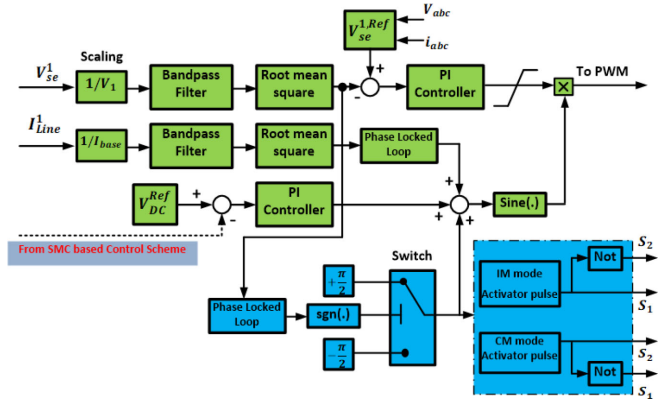

Fig. 5. Proposed control strategy for LPCs.

A. Conventional UIPC Structure

The conventional structure of UIPC has been proposed in [20] and is shown in Fig. 2. As shown, this topology contains three power converters in each phase; VSC_1, $\mathrm{VSC}_2<$, and VSC_3. The first two VSCs, i.e., VSC_1, and VSC_2, are responsible for power exchange control among ac bus and PCC while VSC_3 regulates the ac bus voltage. Also, VSC_1 operates in inductive mode (IM) while VSC_2 operates in capacitive mode (CM). Moreover, each phase needs three power transformers. Therefore, the three-phase model of the conventional UIPC needs nine power converters and nine power transformers [20]. This makes the conventional topology irrationally costly. Furthermore, the dc links of power converters are in parallel and a sturdy control strategy is needed to counteract with dc link voltage fluctuations and prevent malfunction and instability. This issue has not been addressed in [20] and is overcome in the present article.

B. Proposed UIPC Topology

The proposed UIPC is shown in Fig. 3. As demonstrated, each phase includes only one of the line power converter (LPC) which injects series voltage V_{se} through the power transformer T_1 to the transmission line which has the impedance of $R_L + jX_L$ Ω. By injecting this series voltage, as demonstrated in [20], the magnitude of the voltage difference of ac bus and PCC changes that in turn results in changes in power flow between ac bus and dc bus. The phase of the voltage difference is adjusted by the operation of the antiparallel thyristors-based switches S_1 and S_2. When S_1 is on, S_2 is OFF and the UIPC is in IM. When S_2 is on, S_1 is OFF and the UIPC is in CM. Therefore, the phase of the injected series voltage V_{se} can be shifted by $\pm\frac{\pi}{2}$ depending on operation mode the UIPC, which can be IM or CM. Note that in the proposed structure of Fig. 3, there is only one bus power converter (BPC) for all three phases. Through the power transformer T_{BPC}, the BPC regulates the ac bus and also provides bilateral power exchange for the dc microgrid that is connected to the dc bus of the UIPC. It should be noted that in the conventional UIPC structure demonstrated in Fig. 2, the dc bus of the UIPC is connected to a constant capacitor. However, the conventional structure, with too many ILCs, which makes the dc bus unstable in even normal conditions, is not applicable to power flow control among microgrids because the connection of the dc microgrid with a variable output voltage, to this bus makes the dc link unstable. Therefore, this article focuses on the control of the UIPC dc link so that a stable UIPC operation is provided. The overall diagram of the control scheme of the proposed UIPC is shown in Fig. 4. As shown, the controller has two main parts: *LPC control* which should control each LPC accompanied with switches S_1 and S_2, and *observer based SMC dc link control* which should control the nonlinear dc link dynamics and is the main control objective of the present article. The details of the proposed LPC control subsystem are shown in Fig. 5.

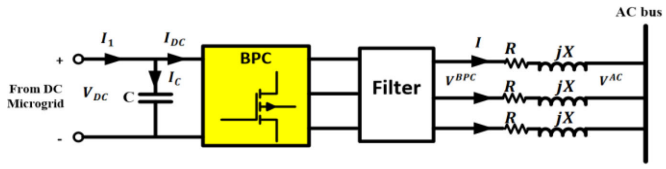

Fig. 6. BPC connected to ac bus and its dc side is supplied by dc microgrid.

Note that in Figs. 4 and 5, a color scheme is used to understand the control communication easier; in these figures, light green is used for LPC and its control scheme, light blue for control of switches S_1 and S_2, and light yellow for BPC and dc link control strategy. In Fig. 5, the voltages and currents of the ac bus and the injected series voltage and the line current are measured and scaled. Then, using bandpass filters, PI controllers, and the dc reference voltage, the pulsewidth modulation pulses are generated for LPCs. The PI controllers have been tuned using genetic algorithm. The phase of the injected series voltage is measured using a phase-locked-loop and controlling the operation mode of the UIPC, i.e., IM or CM, $+\frac{\pi}{2}$ or $-\frac{\pi}{2}$ is applied to the phase of the voltage through switches S_1 and S_2. The control of the BPC is the main control focus of this article and is described in Section III. It should be noted that the power flow equations in the hybrid microgrid when the modified UIPC is used, can be found in [18].

C. Dynamic Model of Nonlinear DC Link and BPC

The BPC model is indicated in Fig. 6. The BPC is connected to ac bus through a harmonic filter and transmission line impedance $R + jX$. The transformer leakage impedance is also included in the line impedance. The BPC dc side is connected to the dc microgrid through capacitor C. $I_{\rm DC}$ is the dc side current, I_C is the capacitor current, and I_1 is the perturbation current due to loads connected to the common dc bus of the dc microgrid. Also, $V^{\rm BPC}$ is the ac output voltage of the BPC and $V^{\rm AC}$ is the ac bus voltage.

Using Kirchhoff's Voltage Law in the BPC ac side and based on dq-transformation, we get

$$V_d^{\rm BPC} = V_d^{\rm AC} + L\left(\frac{dI_d}{dt}\right) + \omega L I_q + I_d R \tag{1}$$

$$V_q^{\rm BPC} = L\left(\frac{dI_q}{dt}\right) - \omega L I_d + I_q R \tag{2}$$

where, ω is the angular frequency in rad/s and L is the line inductance in H. Using Kirchhoff's Current Law in the BPC dc side we have

$$\frac{dV_{\rm DC}}{dt} = \frac{I_1}{C} - \frac{I_{\rm DC}}{C}. \tag{3}$$

Based on power balance equation we get

$$I_{\rm DC} = \frac{1.5 V_d^{\rm AC} I_d}{C V_{\rm DC}}. \tag{4}$$

Substituting (4) in (3) we obtain

$$\frac{dV_{\rm DC}}{dt} = -\frac{1.5 V_d^{\rm AC} I_d}{C V_{\rm DC}} + \frac{I_1}{C}. \tag{5}$$

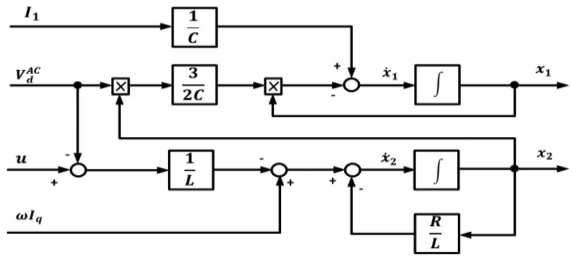

Fig. 7. System representation as a nonlinear dynamic system.

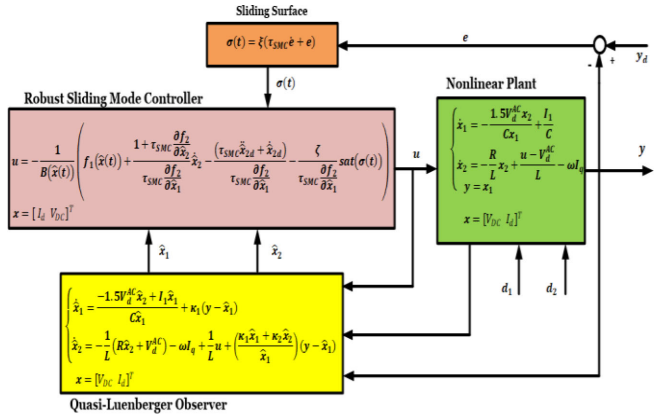

Fig. 8. Proposed observer-based SMC dc link control.

From (1) we have

$$\frac{dI_d}{dt} = -\frac{R}{L} I_d - \omega I_q + \frac{V_d^{\rm BPC} - V_d^{\rm AC}}{L}. \tag{6}$$

Equations (5) and (6) constitute the dynamic model as follows:

$$\begin{cases} \dot{V}_{\rm DC} = -\frac{1.5 V_d^{\rm AC} I_d}{C V_{\rm DC}} + \frac{I_1}{C} \\ \dot{I}_d = -\frac{R}{L} I_d - \omega I_q + \frac{V_d^{\rm BPC} - V_d^{\rm AC}}{L}. \end{cases} \tag{7}$$

Defining the state variable vector $\boldsymbol{x} = [V_{\rm DC} \;\; I_d]^T$, control input $u = V_d^{\rm BPC}$, and output $y = V_{\rm DC}$ we obtain

$$\begin{cases} \dot{x}_1 = -\frac{1.5 V_d^{\rm AC} x_2}{C x_1} + \frac{I_1}{C} \\ \dot{x}_2 = -\frac{R}{L} x_2 + \frac{u - V_d^{\rm AC}}{L} - \omega I_q \\ y = x_1. \end{cases} \tag{8}$$

These equations represent a nonlinear dynamic system and Fig. 7 shows the system as a nonlinear dynamic plant.

III. Proposed Observer-Based SMC DC Link Control Strategy

As described in the previous section, the dc link voltage of the UIPC is fluctuating due to parallel interconnection of multiple power converters, uncertain loads, and dc voltage variation of dc microgrid. Therefore, a robust control strategy is proposed here for the UIPC dc link voltage control as illustrated in Fig. 8. As shown, first the states of the nonlinear dynamic plant are estimated using a Quasi-Luenberger observer. Then, the estimated states are implemented in the robust SMC-based controller that generates the appropriate control signal u for the nonlinear plant.

A. Designing Quasi-Luenberger Observer for Nonlinear Plant

For a nonlinear system of the following form

$$\begin{cases} \dot{x} = f\left(x\left(t\right)\right) + g\left(x\left(t\right)\right)u\left(t\right) \quad ; \quad x\left(0\right) = x_0 \\ y = h\left(x\left(t\right)\right) \end{cases} \tag{9}$$

with the observability matrix

$$Q\left(x\right) = \frac{d}{dx}\begin{bmatrix} h\left(x\right) \\ L_f h\left(x\right) \\ L_f^{n-1} h\left(x\right) \end{bmatrix} \tag{10}$$

where, n is the system order, and $L_f h(x) = \frac{\partial h}{\partial x} f(x)$ is the Lie derivative, there exist an observer as follows:

$$\begin{aligned} \dot{\hat{x}} = f\left(\hat{x}\left(t\right)\right) + g\left(\hat{x}\left(t\right)\right)u\left(t\right) + \left[Q\left(\hat{x}\left(t\right)\right)\right]^{-1}\kappa \\ \times \left[y\left(t\right) - h\left(\hat{x}\left(t\right)\right)\right]\hat{x}\left(0\right) = \bar{x} \end{aligned} \tag{11}$$

where, κ is a gain vector of the form $\kappa = [\kappa_1 \ \ \kappa_2 \ \ldots]$ for a single-input–single-output system (as this is the case here) and a matrix for a multiple-input–multiple-output system and has the properties provided in [23]. To obtain the Quasi-Luenberger observer for the nonlinear plant (8) based on (9)–(11), the steps are as follows.

Step 1: Rewrite the system equations (8) in the standard form of (9) as follows:

$$\begin{cases} \begin{bmatrix} \dot{x}_1 \\ \dot{x}_2 \end{bmatrix} = \underbrace{\begin{bmatrix} -\frac{1.5V_d^{\mathrm{AC}}x_2 + I_1 x_1}{Cx_1} \\ -\frac{1}{L}\left(Rx_2 + V_d^{\mathrm{AC}}\right) - \omega I_q \end{bmatrix}}_{f(x(t))} - \underbrace{\begin{bmatrix} 0 \\ \frac{1}{L} \end{bmatrix}}_{g(x(t))} u\left(t\right) \\ y = h\left(x\right) = x_1. \end{cases} \tag{12}$$

Step 2: The observability matrix is obtained as follows ($n = 2$):

$$\begin{aligned} Q\left(x\right) &= \frac{d}{dx}\begin{bmatrix} h\left(x\right) \\ L_f h\left(x\right) \end{bmatrix} \\ &= \frac{d}{dx}\left[\begin{bmatrix} x_1 \\ \left[0 \quad 1\right]\begin{bmatrix} -\frac{1.5V_d^{\mathrm{AC}}x_2 + I_1 x_1}{Cx_1} \\ -\frac{1}{L}\left(Rx_2 + V_d^{\mathrm{AC}}\right) - \omega I_q \end{bmatrix} \end{bmatrix}\right] \\ &= \begin{bmatrix} 1 & 0 \\ \frac{1.5V_d^{\mathrm{AC}}x_2}{Cx_1^2} & -\frac{1.5V_d^{\mathrm{AC}}}{Cx_1} \end{bmatrix}. \end{aligned} \tag{13}$$

Step 3: The observer dynamics according to (11) are as follows:

$$\dot{\hat{x}}_1 = \frac{-1.5V_d^{\mathrm{AC}}\hat{x}_2 + I_1\hat{x}_1}{C\hat{x}_1} + \kappa_1\left(y - \hat{x}_1\right) \tag{14}$$

$$\begin{aligned} \dot{\hat{x}}_2 = -\frac{1}{L}\left(R\hat{x}_2 + V_d^{\mathrm{AC}}\right) - \omega I_q + \frac{1}{L}u \\ + \left(\frac{\kappa_1\hat{x}_1 + \kappa_2\hat{x}_2}{\hat{x}_1}\right)\left(y - \hat{x}_1\right). \end{aligned} \tag{15}$$

These estimated states are implemented in the SMC-based robust controller, as mentioned before.

B. Designing SMC-Based Robust Controller

In this section, the SMC-based robust controller is designed and applied to the nonlinear plant, as demonstrated in Fig. 8.

Considering the following system [28]:

$$\begin{cases} \dot{x}_1 = f_1\left(x\left(t\right)\right) + b\left(x\left(t\right)\right)u\left(t\right) + d_1 \\ \dot{x}_2 = f_2\left(x\left(t\right)\right) + d_2 \\ y = x_2 \end{cases} \tag{16}$$

where, $\boldsymbol{x} = [x_1 \ \ x_2]^T \subset X \in \mathcal{R}^2$ is the state vector, $u \subset U \in \mathcal{R}$, $|u| \le U_0$ is the control input, $\boldsymbol{d} = [d_1 \ \ d_2]^T$, $|d_1| \le d_{10}$, $|d_2| \le d_{20}$, $|\dot{d}_2| \le \frac{\partial}{\partial t}(d_{20})$, is the disturbance vector, and we have $\frac{\partial f_2}{\partial x_1} \neq 0$, and $B(x) \neq 0$, then we find a switching function $\sigma(t) \in \mathcal{R}$ such that the controller u exists as follows:

$$u = \begin{cases} u^+, \text{ if } \sigma\left(t\right) > 0 \\ u^-, \text{ if } \sigma\left(t\right) < 0. \end{cases} \tag{17}$$

The design steps are as follows.

Step 1: To have the standard form (16), rewrite the system dynamic equations (8) by defining the state vector $\boldsymbol{x} = [\, I_d \ \ V_{\mathrm{DC}}]^T$ and we get

$$\begin{cases} \dot{x}_1 = \underbrace{-\left(\frac{Rx_1 + V_d^{\mathrm{AC}}}{L}\right)}_{f_1(x(t))} + \underbrace{\frac{1}{L}}_{b(x(t))} u\left(t\right) \underbrace{-\omega I_q}_{d_1} \\ \dot{x}_2 = \underbrace{\frac{-1.5V_d^{\mathrm{AC}}x_1}{Cx_2}}_{f_2(x(t))} + \underbrace{\frac{I_1}{C}}_{d_2} \\ y = x_2. \end{cases} \tag{18}$$

Step 2: Define a switching function as follows:

$$\sigma\left(t\right) = \xi\left(\tau_{\mathrm{SMC}}\dot{e} + e\right) \tag{19}$$

where, $e = y - y_d$ is the output error, y_d is the desired output, $\tau_{\mathrm{SMC}} > 0$ is the time constant of the sliding mode, and $\xi > 0$ is a constant parameter. The derivative of this sliding surface is obtained as follows:

$$\dot{\sigma}\left(t\right) = \xi\left(\tau_{SMC}\ddot{e} + \dot{e}\right) = \xi\left(\tau_{SMC}\left(\ddot{x}_2 - \ddot{x}_{2d}\right) + \dot{x}_2 - \dot{x}_{2d}\right) \tag{20}$$

also we have

$$\dot{x}_2 = f_2\left(x\left(t\right)\right) + d_2 \tag{21}$$

$$\begin{aligned} \ddot{x}_2 = \frac{\partial f_2}{\partial x_1}\left(f_1\left(x\left(t\right)\right) + B\left(x\left(t\right)\right)u\left(t\right) + d_1\right) \\ + \frac{\partial f_2}{\partial x_2}\left(f_1\left(x\left(t\right)\right) + d_2\right) + \dot{d}_2. \end{aligned} \tag{22}$$

Substituting (21) and (22) in (20) yields

$$\begin{aligned} \dot{\sigma}\left(t\right) = \xi[\tau_{\mathrm{SMC}}\frac{\partial f_2}{\partial x_1}\left(f_1\left(x\left(t\right)\right) + d_1\right) + \tau_{\mathrm{SMC}}\frac{\partial f_2}{\partial x_2}B\left(x\left(t\right)\right)u\left(t\right) \\ + \left(1 + \tau_{\mathrm{SMC}}\frac{\partial f_2}{\partial x_2}\right)\left(f_2\left(x\left(t\right)\right) + d_2\right) \\ + \tau_{\mathrm{SMC}}\dot{d}_2 - \tau_{\mathrm{SMC}}\ddot{x}_{2d} - \dot{x}_{2d}]. \end{aligned} \tag{23}$$

Step 3: At the sliding surface $\sigma(t) = \dot{\sigma}(t) = 0$ we have

$$B(x(t))\,u_{eq}(t) = -(f_1(x(t)) + d_1) - \frac{1 + \tau_{\rm SMC}\frac{\partial f_2}{\partial x_2}}{\tau_{\rm SMC}\frac{\partial f_2}{\partial x_1}}(f_2(x(t)) + d_2) - \frac{\tau_{\rm SMC}}{\tau_{\rm SMC}\frac{\partial f_2}{\partial x_1}}\dot{d}_2 + \frac{1}{\tau_{SMC}\frac{\partial f_2}{\partial x_1}}(\tau_{\rm SMC}\ddot{x}_{2d} + \dot{x}_{2d}). \quad (24)$$

Step 4: For all $t > t_r$, where t_r is the reaching time, the motion equations are

$$\begin{cases} \dot{x}_1 = -\frac{1+\tau_{\rm SMC}\frac{\partial f_2}{\partial x_2}}{\tau_{\rm SMC}\frac{\partial f_2}{\partial x_1}}\dot{e} + \frac{\tau_{\rm SMC}}{\tau_{\rm SMC}\frac{\partial f_2}{\partial x_1}}\left(-\dot{d}_2 + \ddot{x}_{2d}\right) - \frac{\frac{\partial f_2}{\partial x_2}}{\frac{\partial f_2}{\partial x_1}}\dot{x}_{2d} \\ \dot{e} = -\frac{1}{\tau_{\rm SMC}}e. \end{cases} \quad (25)$$

The time-domain solution of these equations is

$$\begin{cases} x_1(t) = x_1(t_r) + \int_{t_r}^{t} \times \left(-\frac{1+\tau_{\rm SMC}\frac{\partial f_2}{\partial x_2}}{\tau_{\rm SMC}\frac{\partial f_2}{\partial x_1}}\dot{e} + \frac{1}{\frac{\partial f_2}{\partial x_1}}\left(-\dot{d}_2 + \ddot{x}_{2d}\right) - \frac{\frac{\partial f_2}{\partial x_2}}{\frac{\partial f_2}{\partial x_1}}\right)d\tau \\ e = e(t_r)\,e^{-\frac{1}{\tau_{\rm SMC}}(t-t_r)}. \end{cases} \quad (26)$$

Step 5: Controller design: the control input signal is

$$u = u_c + \Delta u \quad (27)$$

where, u_c is the continuous control part, as follows:

$$u_c = -\frac{1}{B(x(t))} \times \left(f_1(x(t)) + \frac{1 + \tau_{\rm SMC}\frac{\partial f_2}{\partial x_2}}{\tau_{\rm SMC}\frac{\partial f_2}{\partial x_1}}\dot{x}_2 - \frac{(\tau_{\rm SMC}\ddot{x}_{2d} + \dot{x}_{2d})}{\tau_{\rm SMC}\frac{\partial f_2}{\partial x_1}}\right) \quad (28)$$

and Δu is the corrective control part as follows:

$$\Delta u = -\frac{1}{B(x(t))}\frac{\zeta}{\tau_{\rm SMC}\frac{\partial f_2}{\partial x_1}}sign(\sigma(t)). \quad (29)$$

In order to reduce the chattering phenomenon, the signum function is replaced by a saturation function as follows:

$$sat(\sigma(t)) = \begin{cases} sign(\sigma(t)) & \text{if} \quad \sigma(t) > \varepsilon \\ \frac{\sigma(t)}{\varepsilon} & \text{if} \quad \sigma(t) \le \varepsilon \end{cases} \quad (30)$$

where, ε is a positive constant that defines the thickness of the boundary layer. Therefore, according to estimated states (14) and (15), obtained using the Quasi-Luenberger observer, the proposed controller is

$$u = -\frac{1}{B(\hat{x}(t))}\left[f_1(\hat{x}(t)) + \frac{1 + \tau_{\rm SMC}\frac{\partial f_2}{\partial \hat{x}_2}}{\tau_{\rm SMC}\frac{\partial f_2}{\partial \hat{x}_1}}\dot{\hat{x}}_2 - \frac{\left(\tau_{\rm SMC}\ddot{\hat{x}}_{2d} + \dot{\hat{x}}_{2d}\right)}{\tau_{\rm SMC}\frac{\partial f_2}{\partial \hat{x}_1}} - \frac{\zeta}{\tau_{\rm SMC}\frac{\partial f_2}{\partial \hat{x}_1}}sat(\sigma(t))\right]. \quad (31)$$

Step 6: Define the Lyapunov function, as follows:

$$V(\sigma(t)) = \frac{1}{2}\sigma(t)^2. \quad (32)$$

Therefore

$$\dot{V}(\sigma(t)) = \sigma(t)\,\dot{\sigma}(t) < 0 \quad (33)$$

$$\sigma(t)\left(\xi\left[\tau_{\rm SMC}\frac{\partial f_2}{\partial x_1}(f_1(x(t)) + d_1) + \tau_{\rm SMC}\frac{\partial f_2}{\partial x_2}B(x(t))\,u(t) + \left(1 + \tau_{\rm SMC}\frac{\partial f_2}{\partial x_2}\right)(f_2(x(t)) + d_2) + \tau_{\rm SMC}\dot{d}_2 - \tau_{\rm SMC}\ddot{x}_{2d} - \dot{x}_{2d}\right]\right) < 0. \quad (34)$$

Using (27)–(30) in (34), we get

$$\sigma(t)\left[\xi\left(\tau_{\rm SMC}\frac{\partial f_2}{\partial \hat{x}_1}d_1 - \zeta sat(\sigma(t)) + \tau_{\rm SMC}\dot{d}_2\right)\right] < 0. \quad (35)$$

Thus;

$$\zeta > d_{10} + \tau_{\rm SMC}\frac{\partial}{\partial t}(d_{20}). \quad (36)$$

Therefore, after a finite reaching time (t_r) the system states reach the sliding surface.

IV. Simulation Results

In this section, the performance of the proposed control scheme for power exchange control among interconnected microgrids in a hybrid microgrid is investigated. Two case studies are considered. The first case illustrates the dynamic performance of the proposed observer-based SMC dc link voltage controller, which is indicated in Fig. 8. The second case shows the power control performance of the modified UIPC equipped with the proposed control strategy. Comparison with the conventional ILCs is also provided in the second case.

A. Performance of Proposed Observer-Based SMC DC Link Voltage Control

The dc link voltage control scheme described in Section II has two main parts. The Quasi-Luenberger state observer and the robust SMC-based controller. The simulation results of the observer and the controller performance applied to the nonlinear dc link plant are illustrated in Figs. 9–16. Figs. 9–14 show the Quai-Luenberger observer achievement in the nonlinear dc link states estimation. The initial states values are $\boldsymbol{x} = [0.12 \quad 0]^T$.

Fig. 9 shows the first true state x_1 versus its estimation $\hat{x}_1$. As shown, the Quai-Luenberger observer is able to successfully estimate the first nonlinear state. The system true state initializes from 0.12 whereas the estimated state arises from zero. The estimation error is shown in Fig. 10. The average value of this error for the nonlinear state x_1 is less than 0.1 and is sufficient for power systems applications. Fig. 11 indicates the estimated second state versus the true state. As shown, the Quasi-Luenberger observer is capable of estimating the second state efficaciously.

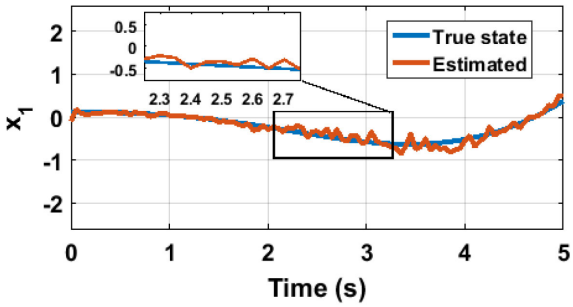

Fig. 9. Estimation of x_1 using Quasi-Luenberger observer.

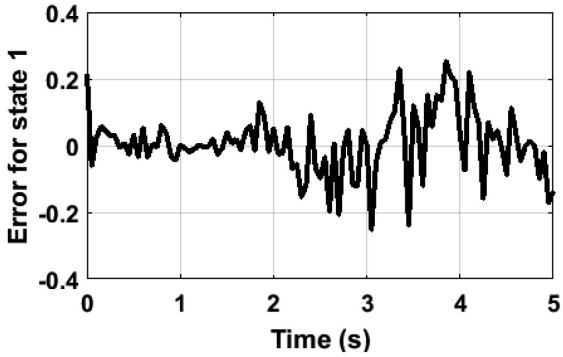

Fig. 10. Estimation error of x_1 using Quasi-Luenberger observer.

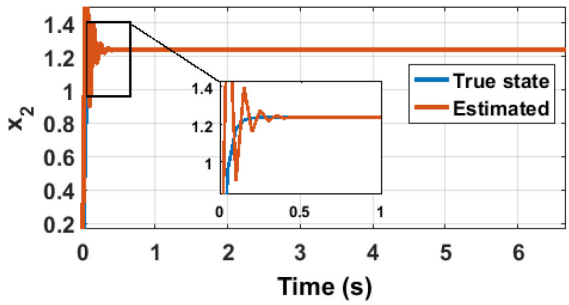

Fig. 11. Estimation of x_2 using Quasi-Luenberger observer.

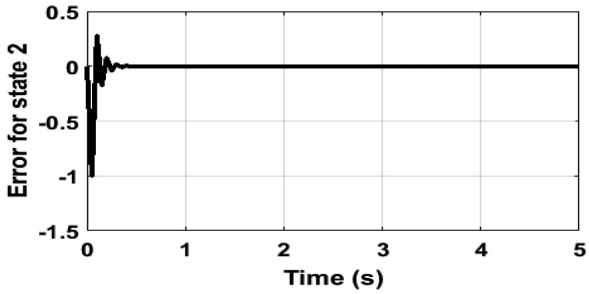

Fig. 12. Estimation error of x_2 using Quasi-Luenberger observer.

After $t = 0.4$ s, the estimated state coincides with true state. The estimation error is illustrated in Fig. 12. This error also goes to zero after $t = 0.4$ s. The normalized correlation is shown in Fig. 13. This value goes to zero after sufficient time, as shown. The key signal of interest used for validating the state estimation is the residuals (or innovations). In this case, the residual analysis

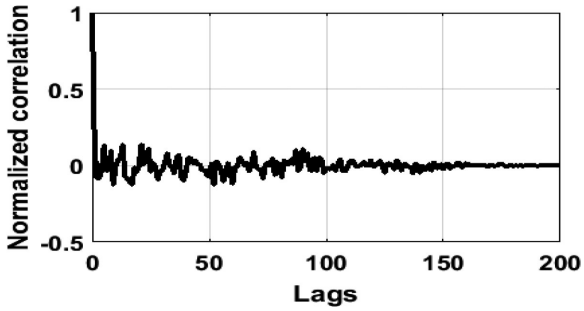

Fig. 13. Normalized correlation.

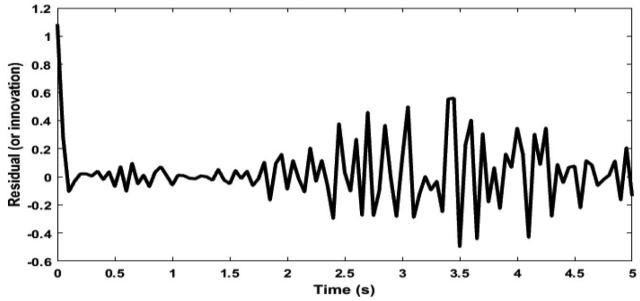

Fig. 14. Residuals.

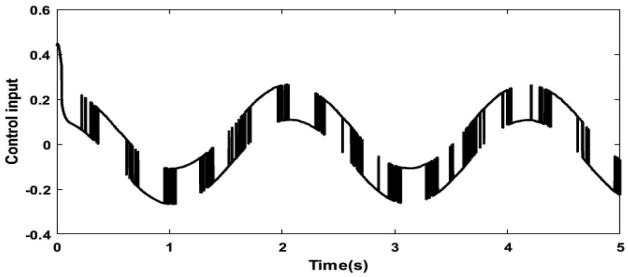

Fig. 15. Control input signal generated by proposed robust controller.

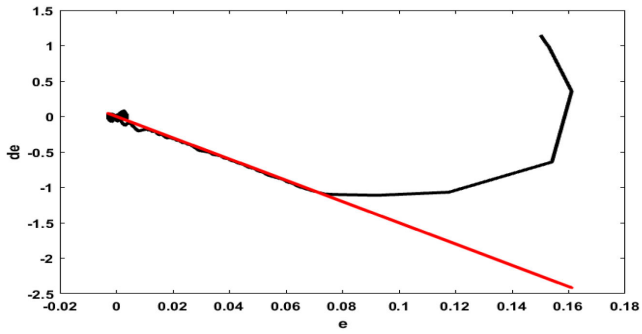

Fig. 16. Sliding surface; system states reach sliding surface at about $t \geq 0.085$ s.

is performed for a single simulation. The residuals are plotted in Fig. 14, which validate the observer performance.

The performance of the proposed robust SMC-based controller is illustrated in Figs. 15 and 16. The generated control signal u is illustrated in Fig. 15. As shown, the proposed control strategy generates a control signal that provides the least possible control effort. The sliding surface is shown in Fig. 16. About

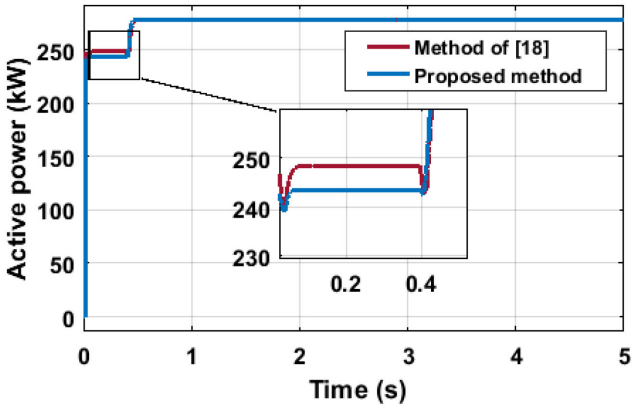

Fig. 17. Scenario1: Active power of dc link of UIPC.

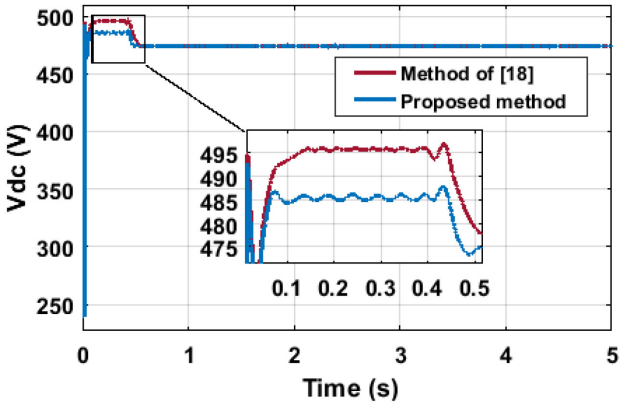

Fig. 18. Scenario1: dc link voltage of UIPC.

$t \geq 0.085$s, the system states will reach the sliding surface and therefore, (36) is satisfied and the closed-loop system is robustly stable.

B. Power Exchange Control Performance

A grid-connected hybrid microgrid including one ac and one dc microgrid is considered. The hybrid microgrid topology is indicated in Fig. 1. The UIPC is equipped with the proposed LPC control scheme shown in Fig. 5 and the proposed observer based-SMC dc link voltage controller illustrated in Fig. 8. The ac microgrid contains 5×50 kW DFIG-based wind turbines which their data can be found in [29]. The dc microgrid includes a 250 kW PV system along with a 50 kW battery. The PV and battery data are given in [30]. We consider two scenarios. In the first scenario, the modified UIPC is used for power exchange control. In the second scenario, the conventional ILCs with the control strategy described in [8] is studied for power exchange control among interconnected microgrids. The hybrid microgrid topology is the same as that of shown in Fig. 1 and is connected to the main power grid. The ac and dc microgrids structures of both scenarios are the same. In two scenarios, the disturbances on the system are changes in load power, and uncertainties of the line parameters.

Scenario 1. Interconnection of Microgrids Using the Modified UIPC: In the first scenario, the proposed UIPC shown in Fig. 3 is applied for power flow control. The nominal value of the dc link voltage is 470 V. This scenario indicates the ability of the proposed observer-based SMC dc link control strategy for occurrence of a change in dc link active power compared to the existing methods in the literature (here the proposed method is benchmarked against the one presented in [18]). The simulation results are shown in Figs. 17 and 18.

The active power of the dc link is illustrated in Fig. 17. In the ac microgrid, three units of the wind turbine generating systems are active. The load in the ac microgrid is equal to 200 kW. Therefore, 50 kW is imported from the main grid to satisfy the ac microgrid loads. The load in the dc microgrid is 250 kW. As shown in Fig. 17, at $t = 0.41$ s, a 30 kW is demanded from the ac microgrid. The exchanged power with the main power grid kept constant. Thus, the dc microgrid is responsible to supply

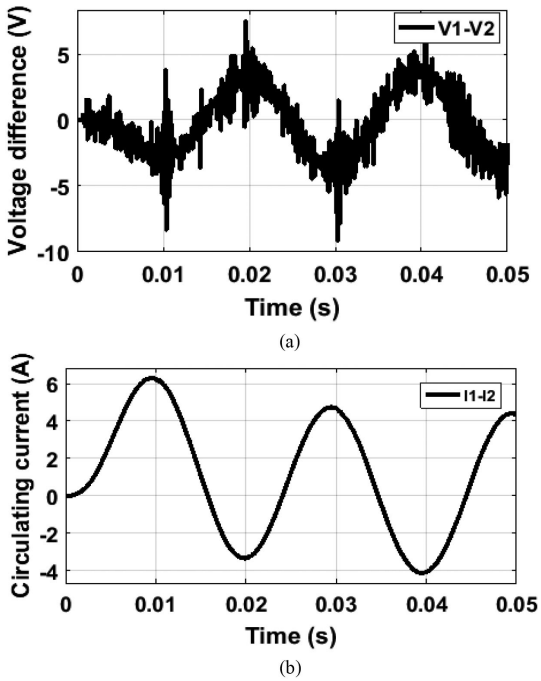

Fig. 19. Voltage and current difference between two ILCs: (a) voltage and (b) current difference (circulating current).

the ac side through the dc link connection of the UIPC. After a transient period of about 0.28 s, with lower ripple as compared to the results of [18], the dc link active power is stabilized and reaches 280 kW indicating the successful operation of the UIPC equipped with the proposed control strategy. The dc link voltage is also shown in Fig. 19. When the power changes, the dc link voltage increases and after a transient period, it reaches the nominal value of 470 V showing the prospering control action of the proposed observer-based SMC dc link controller. The overshoot is less than 5%.

Scenario 2. Interconnection of Microgrids Using Parallel-Connected ILCs: The ILCs are equipped with the control strategy described in [13]. Here, two parallel-connected ILCs are used to connect two microgrids in the grid-connected hybrid microgrid. The power converters parameters are given in [13]. The simulation results are shown in Figs. 19 and 20.

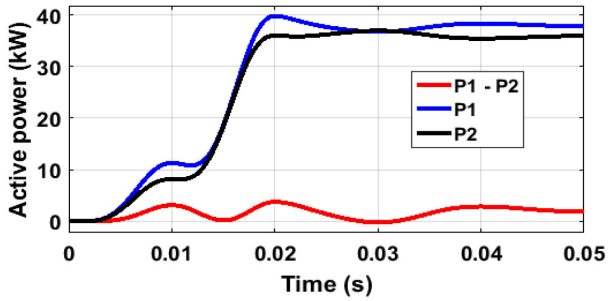

Fig. 20. Active powers of two ILCs.

Fig. 19 shows that when there are uncertainties in the parameters of the transmission lines and loads, and changes in active power, the output voltages of two ILCs differ and cause a circulating current among two ILCs. This in turn results in active power losses indicated in Fig. 20. Similar to Scenario 1, the ac microgrid demand is 50 kW. Therefore, as shown in Fig. 20, the power of ILC 1 and 2 are 38.3 kW and 36.1 kW, respectively. The power difference of these converters is 2.2 kW wasted due to the circulating current.

Comparing the results of both scenarios, one would conclude that the proposed UIPC based power flow control strategy is more effective than the parallel-connected ILCs for interconnecting microgrids in hybrid microgrids since cumbersome paralleling conditions, for example, equal output voltage magnitude, phase angle and frequency, appropriate power sharing among ILCs, etc. (for more information see [18]), are avoided and also circulating current does not appear by using the UIPC. More importantly, since there is not any parallel converter, the power, which has been wasted between the power converters due to the circulating current, is zero.

V. Conclusion

The hybrid microgrids are the most prevalent structure in the smart grids. A hybrid microgrid includes different ac–dc microgrids that are conventionally interconnected through parallel-connected ILCs. In this article, an alternative solution based on a modified UIPC was proposed. A new observer-based SMC strategy was proposed for the dc link voltage control of the UIPC. The simulation results validated the effectiveness of the proposed control strategy in UIPC control under different disturbances. Also, the results showed that the proposed UIPC-based power exchange control is superior over the parallel-connected ILCs since it has no power loss or circulating current appear during different system conditions.

References

[1] X. Chen*et al.*, "Distributed cooperative control of multiple hybrid energy storage systems in a DC microgrid using consensus protocol," *IEEE Trans. Ind. Electron.*, vol. 67, no. 3, pp. 1968–1979, Mar. 2020.

[2] S. Haghifam, K. Zare, and M. Dadashi, "Bi-level operational planning of microgrids with considering demand response technology and contingency analysis," *IET Gener. Transmiss. Distribution*, vol. 13, no. 13, pp. 2721–2730, 2019. [Online]. Available: https://digital-library.theiet.org/content/journals/10.1049/iet-gtd.2018.6516

[3] M. Zolfaghari, R. M. Chabanlo, M. Abedi, and M. Shahidehpour, "A robust distance protection approach for bulk AC power system considering the effects of HVDC interfaced offshore wind units," *IEEE Syst. J.*, vol. 12, no. 4, pp. 3786–3795, Dec. 2018.

[4] P. Lin, T. Zhao, B. Wang, Y. Wang, and P. Wang, "A semi-consensus strategy toward multi-functional hybrid energy storage system in DC microgrids," *IEEE Trans. Energy Convers.*, vol. 35, no. 1, pp. 336–346, Mar. 2020.

[5] Y. Wang, Y. Tang, Y. Xu, and Y. Xu, "A distributed control scheme of thermostatically controlled loads for the building-microgrid community," *IEEE Trans. Sustain. Energy*, vol. 11, no. 1, pp. 350–360, Jan. 2020.

[6] Y. Wang, Y. Xu, Z. Li, T. L. Nguyen, R. Caire, and Q. Tran, "Distributed event-triggered control for islanded microgrids: Cyber-physical design and implementation," in *IEEE/IAS 55th Ind. Commercial Power Syst. Tech. Conf.*, 2019, pp. 1–9.

[7] M. Zolfaghari, M. Abedi, and G. B. Gharehpetian, "Robust nonlinear state feedback control of bidirectional interlink power converters in grid-connected hybrid microgrids," *IEEE Syst. J.*, vol. 14, no. 1, pp. 1117–1124, Mar. 2020.

[8] F. Nejabatkhah, Y. W. Li, and K. Sun, "Parallel three-phase interfacing converters operation under unbalanced voltage in hybrid AC/DC microgrid," *IEEE Trans. Smart Grid*, vol. 9, no. 2, pp. 1310–1322, Mar. 2018.

[9] F. Nejabatkhah and Y. W. Li, "Flexible unbalanced compensation of three-phase distribution system using single-phase distributed generation inverters," *IEEE Trans. Smart Grid*, vol. 10, no. 2, pp. 1845–1857, Mar. 2019.

[10] H. Cai and G. Hu, "Distributed robust hierarchical power sharing control of grid-connected spatially concentrated AC microgrid," *IEEE Trans. Control Syst. Technol.*, vol. 27, no. 3, pp. 1012–1022, May 2019.

[11] S. A. Taher and M. Zolfaghari, "Designing robust controller to improve current-sharing for parallel-connected inverter-based DGs considering line impedance impact in microgrid networks," *Int. J. Elect. Power Energy Syst.*, vol. 63, pp. 625–644, 2014.

[12] X. Lu, J. Guerrero, R. Teodorescu, T. Kerekes, K. Sun, and L. Huang, "Control of parallel-connected bidirectional AC-DC converters in stationary frame for microgrid application," in *IEEE Energy Convers. Congr. Expo.*, 2011, pp. 4153–4160.

[13] F. Wang, J. L. Duarte, and M. A. M. Hendrix, "Design and analysis of active power control strategies for distributed generation inverters under unbalanced grid faults," *IET Gener. Transmiss. Distribution*, vol. 4, no. 8, pp. 905–916, 2010.

[14] X. Zhang, K. Hengster-Movrić, M. Šebek, W. Desmet, and C. Faria, "Distributed observer and controller design for spatially interconnected systems," *IEEE Trans. Control Syst. Technol.*, vol. 27, no. 1, pp. 1–13, Jan. 2019.

[15] M. Ouassaid, M. Maaroufi, and M. Cherkaoui, "Observer-based nonlinear control of power system using sliding mode control strategy," *Electric Power Syst. Res.*, vol. 84, no. 1, pp. 135–143, 2012.

[16] A. S. L. V. Tummala, R. Inapakurthi, and P. V. Ramanarao, "Observer based sliding mode frequency control for multi-machine power systems with high renewable energy," *J. Modern Power Syst. Clean Energy*, vol. 6, no. 3, pp. 473–481, 2018.

[17] Y. Liu, Q. H. Wu, X. X. Zhou, and L. Jiang, "Perturbation observer based multiloop control for the DFIG-WT in multimachine power system," *IEEE Trans. Power Syst.*, vol. 29, no. 6, pp. 2905–2915, Nov. 2014.

[18] M. Zolfaghari, M. Abedi, and G. B. Gharehpetian, "Power flow control of interconnected ac-dc microgrids in grid-connected hybrid microgrids using modified UIPC," *IEEE Trans. Smart Grid*, vol. 10, no. 6, pp. 6298–6307, Nov. 2019.

[19] M. Zolfaghari, M. Abedi, and G. B. Gharehpetian, "Power exchange control of clusters of multiple AC and DC microgrids interconnected by UIPC in hybrid microgrids," in *24th Electr. Power Distribution Conf.*, 2019, pp. 22–26.

[20] J. Pourhossein, G. B. Gharehpetian, and S. H. Fathi, "Unified interphase power controller (UIPC) modeling and its comparison with IPC and UPFC," *IEEE Trans. Power Del.*, vol. 27, no. 4, pp. 1956–1963, Oct. 2012.

[21] M. Firouzi, G. B. Gharehpetian, and Y. Salami, "Active and reactive power control of wind farm for enhancement transient stability of multi-machine power system using UIPC," *IET Renewable Power Gener.*, vol. 11, no. 8, pp. 1246–1252, 2017.

[22] M. Firouzi, G. B. Gharehpetian, and B. Mozafari, "Power-flow control and short-circuit current limitation of wind farms using unified interphase power controller," *IEEE Trans. Power Del.*, vol. 32, no. 1, pp. 62–71, Feb. 2017.

[23] G. Ciccarella, M. Dalla Mora, and A. Germani, "A luenberger-like observer for nonlinear systems," *Int. J. Control*, vol. 57, no. 3, pp. 537–556, 1993.

Mahdi Zolfaghari (Member, IEEE) was born in Aleshtar, Lorestan, Iran, in 1987. He received the Ph.D. degree (Hons.) in electrical power engineering from the Department of Electrical Engineering, Amirkabir University of Technology (formerly, Tehran Polytechnic), Tehran, Iran, in 2019.

He is currently a Postdoctoral Research Fellow with the Amirkabir University of Technology, Tehran, Iran, with the support of Elite National Foundation of Iran. He has authored or coauthored four technical books and more than 25 papers. His research interests include smart grids, renewable energy, analysis and robust control of complex and uncertain systems.

Dr. Zolfaghari is a member of the Iranian Inventors Association. He also acts as an Editor for the *Journal of Advanced Research in Electrical and Electronics Engineering*, Australia, and the *Journal of Hydro Science & Marine Engineering*, Singapore.

Gevork B. Gharehpetian (Senior Member, IEEE) received the B.S. degree in electrical engineering from Tabriz University, Tabriz, Iran, in 1987, the M.S. degree in electrical engineering from the Amirkabir University of Technology, Tehran, Iran, in 1989, and the Ph.D. degree in electrical engineering from Tehran University, Tehran, Iran, in 1996.

He has authored or coauthored more than 1200 journal and conference papers. His research interests include smart grid, microgrids, Flexible AC Transmission System (FACTS) and high voltage direct current systems, monitoring of power transformers and its transients.

Prof. Gharehpetian was selected as the Distinguished Professor of Iran by the Ministry of Science Research and Technology (SMRT), the Best Researcher of Iran in the field of energy by Iran Energy Association, the Distinguished Researcher of Iran by the SMRT, the Distinguished Professor of electrical engineering by the Academy of Science of the Islamic Republic of Iran, the laureates of Alameh Tabatabaei Award by National Elites Foundation. He was the recipient of the National Prize in 2008, 2010, 2018, 2018, 2019, and 2019, respectively. Based on the Web of Science database (2005–2015), he is among the world's top 1% elite scientists according to Essential Science Indicators ranking system.

Amjad Anvari-Moghaddam (Senior Member, IEEE) received the Ph.D. degree (Hons.) in power systems engineering from the University of Tehran, Tehran, Iran, in 2015.

He is currently an Associate Professor with the Department of Energy Technology, Aalborg University, Aalborg, Denmark. His research interests include planning, control, and operation of energy systems, mostly renewable and hybrid power systems with appropriate market mechanisms.

Dr. Anvari-Moghaddam is currently the Associate Editor of the IEEE TRANSACTIONS ON POWER SYSTEMS, IEEE ACCESS, IEEE OPEN ACCESS JOURNAL OF POWER AND ENERGY, IEEE POWER ENGINEERING LETTERS, *IET Renewable Power Generation*, *International Transactions on Electrical Energy Systems*, and Lead Guest Editor of the IEEE TRANSACTIONS ON INDUSTRIAL INFORMATICS, *Journal of Future Generation Computer Systems*, *Applied Thermal Engineering*, as well as *Applied Sciences, Electronics, and Sustainability*. He was the recipient of 2020 DUO—India Fellowship Award, the 2018 IEEE Outstanding Leadership Award (Halifax, Nova Scotia, Canada), the 2017 IEEE Outstanding Service Award (Exeter-UK), and the DANIDA research grant from the Ministry of Foreign Affairs of Denmark in 2018.